

## Comparative Evaluation of MMPBSA and XSCORE To Compute Binding Free Energy in XIAP–Peptide Complexes

Cristian Obiol-Pardo and Jaime Rubio-Martinez\*

Departament Química Física, Universitat de Barcelona (UB), Martí i Franqués 1, E-08028 Barcelona, Spain

Received September 21, 2006

Evaluation of binding free energy in receptor–ligand complexes is one of the most important challenges in theoretical drug design. Free energy is directly correlated to the thermodynamic affinity constant, and, as a first step in druglikeness, a lead compound must have this constant in the range of micro- to nanomolar activity. Many efforts have been made to calculate it by rigorous computational approaches, such as free energy perturbation or linear response approximation. However, these methods are still computationally expensive. We focus our work on XIAP, an antiapoptotic protein whose inhibition can lead to new drugs against cancer disease. We report here a comparative evaluation of two completely different methodologies to estimate binding free energy, MMPBSA (a force field based function) and XSCORE (an empirical scoring function), in seven XIAP–peptide complexes using a representative set of structures generated by previous molecular dynamics simulations. Both methods are able to predict the experimental binding free energy with acceptable errors, but if one needs to identify slight differences upon binding, MMPBSA performs better, although XSCORE is not a bad choice taking into account the low computational cost of this method.

### INTRODUCTION

Protein–protein interactions<sup>1</sup> are crucial for many biological processes, such as signal transduction or protein inhibition. However, because these interactions are usually distributed along a big and flat surface, the design of small molecules to disrupt them is an unusual approach in drug discovery.<sup>2</sup> Peptides, although not having all the desirable druglike properties, can be a good first approach in a drug design process because they are able to cover a large interaction surface area. Thus, understanding protein–peptide recognition at its atomic and energetic levels is extremely important.

With the advent of faster and cheaper computers, structure-based drug design has become an important step toward a fast and efficient drug discovery project. In this scenario, molecular docking appears as a fundamental tool that consists basically of two major tasks: the generation of all accessible conformations and their ranking in order to identify the bioactive one. As effectiveness of molecular docking is strongly dependent on the scoring function used, many efforts have been made to estimate binding free energy of protein–ligand complexes by computational approaches. Thus, free energy perturbation<sup>3</sup> or linear response approximations<sup>4</sup> are rigorous methods that consider the solvent explicitly. However, they are still computationally expensive to study a large and diverse set of protein–ligand or protein–peptide systems.

During the last years, different approaches have been described as cheaper alternatives to the estimation of binding free energy in a fast and more or less accurate form.

A widely used force field scoring function is MMPBSA (Molecular Mechanics Poisson Boltzmann Surface Area).<sup>5</sup> Usually, this approach computes binding free energy by using

a set of conformations for the complex, the ligand and the receptor taken from one molecular dynamics trajectory, together with a continuum solvent model. It has been evaluated with remarkable success in numerous and very different systems such as protein–ligand or RNA–ligand complexes.<sup>6,7</sup> This function can be classified as *ab initio*, in the sense that no experimental results are used for global evaluation, although they have been taken into account for the obtainment of some terms involved in its calculation.

On the other hand, XSCORE<sup>8</sup> is an experimental scoring function as it is calibrated with experimental information. It takes into account van der Waals interactions, hydrogen bonding, deformation penalty, and hydrophobic effects between the receptor and the ligand. This function was able to predict the binding free energy with a small deviation of 2.2 kcal/mol in a set of 30 protein–ligand complexes.<sup>8</sup> It has recently been evaluated in comparison with 10 different scoring functions<sup>9</sup> by using an exhaustive conformational sampling. Results indicate that XSCORE has an acceptable success rate for molecular docking tasks and binding free energy prediction in protein–ligand systems. This method is computationally very cheap, and it has been developed to treat a large set of ligands within a rigid receptor structure approach.

Both methodologies, XSCORE and MMPBSA, are able to provide clear physical meaning of the suitable ligand features for the inhibition of a protein. The first one can provide a number of hydrogen bonds, hydrophobic zones, or a number of frozen rotatable bonds during the binding process, among others. The second one can provide electrostatic, van der Waals, and solvation contributions to the binding process.

We report here a comparative evaluation between both methods to estimate the binding free energy of seven protein–peptide complexes with biological relevance.

\* Corresponding author phone: 0034-934039263; fax: 0034-934021231; e-mail: jaime.rubio@ub.edu

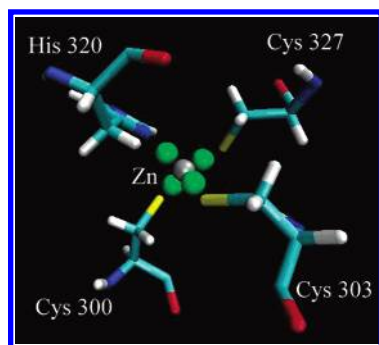


**Figure 1.** Tetrahedral structure of dummy atoms and zinc in XIAP.

These complexes are formed by the well-known X-linked inhibitor of apoptosis protein (XIAP), related to the progress and resistance of tumors to conventional treatments,<sup>10–12</sup> with seven inhibitor peptides, one of them being the 9-residue peptide derived from Smac/DIABLO protein, a natural inhibitor of the XIAP protein. The remaining six ones are 4-residue peptides derived from the Smac/DIABLO AVPI sequence in a wide range of experimental affinities,<sup>13</sup> ranging from micro- to nanomolar. Many recent experimental studies have been devoted to the development of potent inhibitors of XIAP based mainly on the 4-residue sequence of the Smac/DIABLO.<sup>14–16</sup> So it is interesting to find a fast and reliable theoretical method for the reproduction of available experimental affinities and the prediction of new ones.

## METHODS

**Construction of the XIAP–Smac/DIABLO(9 Residues) Complex.** The initial 3D structure of the human XIAP–Smac/DIABLO(9) complex was taken from the Protein Data Bank (PDB entry 1G3F).<sup>17</sup> The complex is formed by the BIR3 domain of the XIAP protein (residues 240–357) and nine nitrogen terminal residues of the Smac/DIABLO protein (residues 1–9, AVPIAQKSE sequence). The cationic dummy approach<sup>18</sup> was used for the treatment of the zinc atom of the XIAP protein. In this method, four dummy atoms are used to impose tetrahedral orientation required for zinc ligands (see Figure 1). This method was employed with remarkable success in farnesyltransferase,<sup>18</sup> matrix metalloproteinase,<sup>19</sup> phosphotriesterase,<sup>20</sup> and beta-lactamase.<sup>21</sup> It solves the problem of maintaining the tetrahedral coordination of the metal throughout a molecular dynamics simulation without the loss of protein flexibility. The zinc atom is bounded covalently to the dummies and interacts with the protein only by van der Waals forces, while the dummies interact with the protein only by electrostatics. A cubic box of 8243 TIP3P waters<sup>22</sup> was added to the system to perform the molecular dynamics simulation in explicit solvent. No counterions were added except for a uniform plasma neutralizing the system, as implemented in AMBER package.

**Construction of the XIAP–Peptides (4 Residues) Complexes.** Six XIAP–peptide(4) complexes were modeled straight from the coordinates of the first complex cutting the five carbon terminal residues of Smac/DIABLO. Then, initial coordinates of main chain atoms are always the same for all designed peptides. In this form, conformational sampling begins with the expected bioactive conformation. Appropriate point mutations for lateral chains were done when required. These peptides are AVPI (simply the four first residues),

ARPF, AGPI, AVPA, AVPY, and AVPE. In the same way, the cationic dummy approach was used for the zinc atom present in XIAP. A cubic box of approximately 8000 TIP3P waters<sup>22</sup> was added to each system to perform molecular dynamics simulations in explicit solvent. No counterions were added except for a uniform plasma neutralizing the system, as implemented in AMBER package.

**Minimization and Molecular Dynamics.** All the calculations were carried out at molecular mechanics level using the parm94<sup>23</sup> force field as implemented in the AMBER-7 suite of programs.<sup>24</sup> The solvent was considered explicitly, and the cutoff distance was kept to 9 Å to compute the nonbonded interactions. All simulations were performed under periodic boundary conditions, and long-range electrostatics were treated by using the particle-mesh-Ewald method.<sup>25</sup>

The seven complexes were energy minimized to remove possible steric stress by a multistep procedure. First, water molecules were allowed to relax, while the rest of the system was kept frozen. Second, side chains of XIAP and peptides were relaxed as well as water molecules. Third, all atoms except zinc, dummies, and the four coordinated residues of XIAP were relaxed, and finally all atoms were allowed to move. We used the steepest descent method followed by the conjugated gradient method to achieve energy gradients lower than 1 kcal/mol, which are reasonable gradients for local minimums and good structures to start the molecular dynamics trajectory.

Molecular dynamics for the complexes were performed at constant temperature by coupling the systems to a thermal bath using Berendsen's algorithm,<sup>26</sup> with a time coupling constant of 0.2 ps. The time integration step was set to 1 fs, and the list of nearest neighbor atoms was updated every 15 steps. A cutoff distance of 9 Å was used. All bond lengths were constrained with the SHAKE algorithm<sup>27</sup> to achieve a rapid energy convergence.

Molecular dynamics began by heating up each of the minimized systems to 300 K at a constant rate of 30 K/10 ps constraining the protein atoms. The second step consisted of a 40 ps pressure-constant period to raise the density while still keeping the protein atoms constrained. The third step was a 150 ps volume-constant period with only the zinc, dummies, and four coordinated residues constrained. Finally, 1 ns dynamics calculations were performed for each free system in the NVT ensemble at a constant temperature of 300 K.

Once the total energy of the systems was equilibrated, 100 time-equidistant snapshots were taken out from MD production of each XIAP–peptide complex. After removing water molecules, structures were used for the evaluation of binding free energies.

**XSCORE.** XSCORE<sup>8</sup> is an empirical scoring function that computes the binding free energy with the following terms:

$$\Delta G_{\text{bind}} = \Delta G_{\text{vdw}} + \Delta G_{\text{H-bond}} + \Delta G_{\text{deformation}} + \Delta G_{\text{hydrophobic}} + \Delta G_0 \quad (1)$$

Here,  $\Delta G_{\text{vdw}}$  accounts for the van der Waals interactions between the receptor and the ligand,  $\Delta G_{\text{H-bond}}$  accounts for the hydrogen bonding between the receptor and the ligand,  $\Delta G_{\text{deformation}}$  accounts for the deformation penalty (number of ligand rotatable bonds frozen during the binding process),

$\Delta G_{\text{hydrophobic}}$  accounts for the hydrophobic effect with three different algorithms (HS, HP, and HM), the HP, HM, and HS terms are related to optimum distances of hydrophobic contacts, to the environment of hydrophobic ligand atoms into the receptor, and to the surface accessible area, respectively, and  $\Delta G_0$  is a regression constant. Finally, the binding affinity of a given protein–ligand complex is expressed in  $\text{p}K_d$  units, with  $K_d$  being the dissociation constant ( $\text{p}K_d = -\log K_d$ ). Detailed information about how these terms have been obtained can be read in the original reference.<sup>8</sup> Regression constants in the present work were not altered from the original XSCORE function, and version 1.2 of the program was used.

XSCORE was evaluated for each of the 100 extracted structures for each of the XIAP–peptide complexes. Thus, conformational changes of the receptor, which is used as a rigid structure in XSCORE calculations, have now been taken into account.

**MMPBSA.** MMPBSA (Molecular Mechanics Poisson Boltzmann Surface Area)<sup>5</sup> computes the binding free energy by using a thermodynamic path that includes the solvation contribution. The following expression now is used to describe the binding free energy:

$$\Delta G_{\text{bind}} = \Delta G_{\text{bind}}^0 + \Delta G_{\text{RL}}^{0 \rightarrow \text{sol}} - \Delta G_{\text{R}}^{0 \rightarrow \text{sol}} - \Delta G_{\text{L}}^{0 \rightarrow \text{sol}} \quad (2)$$

Here,  $\Delta G_{\text{bind}}^0$  accounts for the free energy of binding in vacuo, and the rest of the terms are the solvation free energy of the receptor–ligand complex (RL), receptor (R), and ligand (L).

$\Delta G_{\text{bind}}^0$  is decomposed into enthalpic plus entropic contributions, the first one being computed by the total energy of the force field and the second one computed usually by a normal-mode analysis.<sup>28</sup>

The estimation of entropic contributions is computationally intensive. For this reason, normal mode computations are carried out in the absence of water, with a distance dependent dielectric constant ( $\epsilon=4r$ ) and using a reduced system including only those protein atoms located within a pre-defined cutoff from the ligand atoms. The structures of the subsystems are minimized to a given gradient, and the vibrational frequencies are computed for each of them. Moreover, for entropic estimation, it is widely accepted to work with only a few structures from the dynamics run, due the computational cost, while the rest of the terms are statistically balanced using about 100 structures.

Each term of the solvation part of eq 2 is decomposed as follows

$$\Delta G^{0 \rightarrow \text{sol}} = \Delta G_{\text{ele}}^{0 \rightarrow \text{sol}} + \Delta G_{\text{np}}^{0 \rightarrow \text{sol}} \quad (3)$$

where  $\Delta G_{\text{ele}}^{0 \rightarrow \text{sol}}$  accounts for the electrostatic contribution to solvation. This term is obtained, as implemented in the MEAD program,<sup>29</sup> by solving the linear Poisson Boltzmann equation in a continuum model of the solvent by the finite difference algorithm<sup>30</sup> using a 0.5 Å grid extended 20% beyond the solute.  $\Delta G_{\text{np}}^{0 \rightarrow \text{sol}}$  accounts for the nonpolar contribution to solvation, related linearly to the solvent accessible surface area (SASA),<sup>31</sup> computed in the present work through the LCPO method<sup>32</sup>

$$\Delta G_{\text{np}}^{0 \rightarrow \text{sol}} = a\text{SASA} + b \quad (4)$$

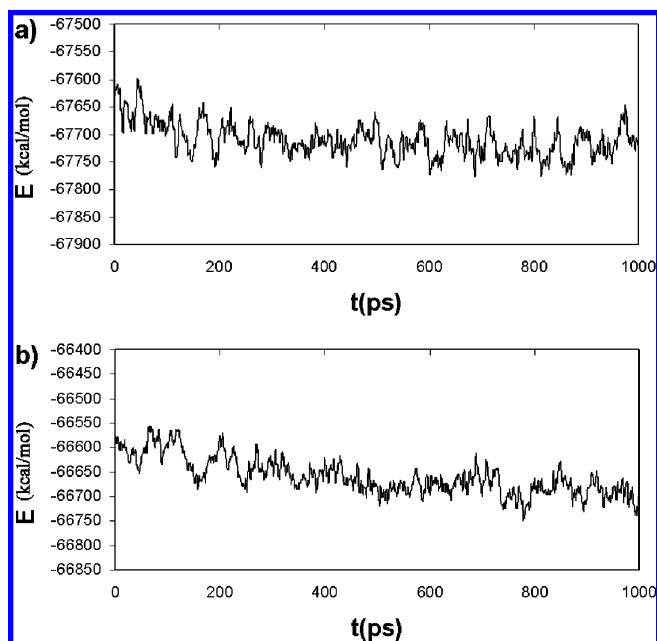
with  $a = 0.00542 \text{ kcal}/(\text{mol} \text{ \AA}^2)$  and  $b = 0.92 \text{ kcal/mol}$ . Parse radii were used for all atoms except for  $\text{Zn}^{2+}$ , which was used 2.0 Å.<sup>33</sup> For the calculation of  $\Delta G_{\text{bind}}^0$  a parm99  $\text{Zn}^{2+}$  was used.<sup>34</sup> All other constants of the MMPBSA methodology are set to standard values.

MMPBSA was performed using 100 snapshots obtained for each XIAP–peptide complex. Coordinates given by the complex structures were used to generate a separate set of structures for the XIAP and for the peptides, thus we use the one-trajectory protocol. This approximation avoids the calculation of separated trajectories for XIAP and peptides alone and supposes a little conformational change of the fragments. This approximation is always a source of error because some changes are expected upon binding especially for peptide ligands. However, this approximation is necessary in order to work in a similar way when compared with XSCORE methodology, where conformational changes of the fragments upon binding cannot be taken into account.

## RESULTS AND DISCUSSION

The evolution of the total energy for the XIAP–Smac/DIABLO(9 residues) and XIAP–AVPY systems versus time throughout their molecular dynamics trajectories is shown in Figure 2. The first complex achieves a rapid convergence in the first 200 ps, while the XIAP–AVPY complex needs about 500 ps to achieve energy convergence. All other XIAP–peptide complexes showed the same behavior. The different convergence rates is a reflection of the fact that initial conformation for the XIAP/Smac/DIABLO complex comes from a NMR structure, while the rest were obtained by homology modeling.

Table 1 sets the experimental and averaged Zn-coordinated atom distances during the dynamics for the XIAP–Smac/DIABLO complex. It can be seen as a good agreement with respect to the experimental ones.<sup>17</sup> Similar results were obtained for the other XIAP–peptide complexes. Thus, the

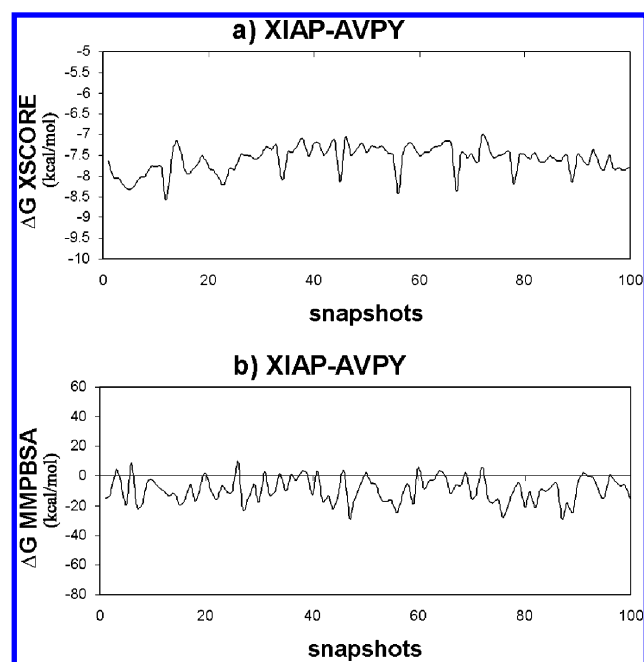


**Figure 2.** Evolution of total energy versus time for (a) the XIAP–Smac/DIABLO(9res) complex and (b) the XIAP–AVPY complex.



**Table 1.** Experimental and Average Distances and Angles of the Zinc-Coordinated Atoms in the XIAP–Smac/DIABLO Complex<sup>a</sup>

	exptl distance (Å)	av distance (Å)
Zn–S(Cys 300)	2.10	2.12 (0.04)
Zn–S(Cys 303)	2.10	2.13 (0.04)
Zn–S(Cys 327)	2.10	2.14 (0.04)
Zn–N(His 320)	2.21	2.07 (0.05)
	exptl angle (deg)	av angle (deg)
S(Cys 300)–Zn–S(Cys 327)	108.5	113.9 (5.1)
S(Cys 300)–Zn–N(His 320)	107.2	105.7 (4.6)
S(Cys 300)–Zn–S(Cys 303)	107.5	106.1 (4.5)
S(Cys 303)–Zn–N(His 320)	113.1	113.8 (5.6)
S(Cys 303)–Zn–S(Cys 327)	108.6	111.4 (4.6)
S(Cys 327)–Zn–N(His 320)	111.7	101.7 (4.3)

<sup>a</sup> Standard deviation is in brackets.**Figure 3.** Evolution of binding free energy versus time for the XIAP–AVPY complex using (a) the XSCORE method and (b) the MMPBSA method.

cationic dummy atom approach has proved its suitability for the molecular dynamic study of these systems.

Accordingly, 100 structures of receptor and ligand were extracted from the production period of the 1 ns molecular dynamics trajectories, one snapshot each 8 ps for the last 800 ps for the experimental complex or one snapshot each 5 ps for the last 500 ps for the other complexes, and prepared for the evaluation of the binding free energy using XSCORE and MMPBSA methods. As described before, water molecules were removed from every snapshot.

Figure 3 shows the evolution of the binding free energy versus time (or snapshots) using both methods for the XIAP–AVPY system taken as an example (in MMPBSA the entropic estimation is not included). As can be seen, the property is well time stabilized. However, free energy fluctuation is about 0.4 kcal/mol for the XSCORE methods, while it is much greater in the MMPBSA methodology (5.0 kcal/mol). Moreover, it gives negative and positive binding free energy values. This is an important fact, in the sense that for the first method, all molecular dynamics conformations show very close energies, while for the second slight

changes in conformations are translated in great differences in binding, so this method seems more capable of identifying which peptides fit better in the binding pocket. The same behavior was noticed for the other systems.

Table 2 lists the average results of the binding free energy calculations and the different energy contributions as the XSCORE function gives. The VDW term accounts for the van der Waals energy between the fragments computed with an 8–6 Lennard Jones potential. The HB term accounts for the number of optimal hydrogen bonds between the fragments. The HP, HM, and HS terms account for hydrophobic effects and are related to optimum distances of hydrophobic contacts, to the environment of hydrophobic ligand atoms into the receptor, and to the surface accessible area, respectively. Finally, the RT term denotes the rotor or number of rotatable bonds predictably frozen during binding. The four following columns are the three scoring functions, HPScore, HMScore, and HSScore, depending on which hydrophobic effect has been taken into account, and the final XSCORE value as the average of the three scoring functions (in  $pK_d$  units). The last two columns show the calculated binding free energy and the experimental one in kcal/mol, using the relationship between the dissociation constant and free energy at 300 K.

XSCORE results are, in all cases, lower than the experimental ones with ARPF showing the highest error, 3 kcal/mol. XSCORE overscores low affinity peptides and underscores high affinity peptides, being all the calculated binding free energies in a reduced range of 0.44 kcal/mol, with the XIAP–Smac/DIABLO(9) complex as the only exception. This fact was noted previously when studying other protein–nonpeptide complexes.<sup>35</sup> The authors suggest that this is caused in part by a lack of enough penalty terms in XSCORE being the only one to count the number of rotatable bonds. Within this range XSCORE is not able to separate the most active ligands (XIAP–Smac/DIABLO, AVPI, ARPF, and AVPY) from the least active ones (AGPI, AVPA, and AVPE), which are orders of magnitude less active. So, the correlation coefficient is very small, only 0.02, which is a poor method performance.

Therefore, despite the fact that this empirical scoring function estimates the binding free energy within 1–3 kcal/mol in a few minutes on a standard computer, it cannot be used to distinguish the most active ligands from the least active ones for the systems studied here, at least in its original form. Moreover, the AVPI peptide is predicted to have the highest affinity in contradiction to the experimental results.

However, it gives some insights into the ligand features, thus we see 3–4 intermolecular hydrogen bonds in all peptides and 6–24 frozen rotatable bonds during the binding process. One can analyze also what atoms are responsible for hydrogen bonds and the most important van der Waals contacts in each ligand if it is needed.

As XSCORE is composed of three functions, we can separately analyze each of them in order to see its performance when working alone. Table 3 shows the calculated binding free energy taking only into account one of the functions. Regarding the correlation coefficients, all three functions alone work better than the average final score, but HMScore gives the best results, having a correlation coefficient of 0.58 which is a good result for a scoring function.<sup>35</sup> Unfortunately, none of them is still able to clearly identify

**Table 2.** Average Data of XSCORE Methodology<sup>a</sup>

	VDW	HB	HP	HM	HS	RT	HP Score	HM Score	HS Score	X SCORE	$\Delta G_{\text{XSCORE}}$ (kcal/mol)	$\Delta G_{\text{bind,exp}}$ (kcal/mol)
XIAP–Smac/DIABLO(9res)	460.3	3.7	53.4	5.86	261.1	24	4.61	5.71	4.28	4.86	−6.67 (0.18)	−8.78
XIAP–AVPI	395.1	3.3	42.4	3.48	240.8	7	5.24	6.15	5.47	5.62	−7.71 (0.17)	−8.67
XIAP–ARPF	447.8	3.8	44.7	3.45	184.9	10	5.30	6.08	5.20	5.53	−7.59 (0.40)	−10.56
XIAP–AGPI	400.7	4.0	40.7	2.34	202.9	7	5.28	5.80	5.40	5.49	−7.53 (0.19)	−5.95
XIAP–AVPA	348.2	3.0	33.2	2.95	171.2	6	5.00	5.83	5.08	5.3	−7.27 (0.17)	−6.66
XIAP–AVPY	382.7	3.7	43.2	3.85	190.5	7	5.22	6.29	5.25	5.59	−7.67 (0.34)	−8.95
XIAP–AVPE	419.3	4.1	38.2	2.45	176.5	8	5.27	5.82	5.28	5.46	−7.49 (0.17)	−5.53

<sup>a</sup> VDW accounts for van der Waals interaction, HB are the number of hydrogen bonds found, HP, HM, and HS account for the hydrophobic effect, RT are the number of rotatable bonds of each ligand, HPScore, HMScore, and HSScore are the three scoring functions, XSCORE is the average HPScore, HMScore, and HSScore,  $\Delta G_{\text{XSCORE}}$  is the binding free energy by using the XSCORE method with its standard deviation in brackets, and finally  $\Delta G_{\text{bind,exp}}$  accounts for the experimental binding free energy.

**Table 3.** Average Data of the Three Scoring Functions Included in XSCORE with Its Standard Deviation in Brackets<sup>a</sup>

	$\Delta G_{\text{HPScore}}$	$\Delta G_{\text{HMScore}}$	$\Delta G_{\text{HSScore}}$	$\Delta G_{\text{bind,exp}}$
XIAP–Smac/DIABLO(9res)	−6.32 (0.21)	−7.83 (0.17)	−5.87 (0.18)	−8.78
XIAP–AVPI	−7.19 (0.19)	−8.44 (0.14)	−7.50 (0.18)	−8.67
XIAP–ARPF	−7.27 (0.45)	−8.34 (0.38)	−7.13 (0.41)	−10.56
XIAP–AGPI	−7.24 (0.19)	−7.96 (0.18)	−7.41 (0.20)	−5.95
XIAP–AVPA	−6.86 (0.19)	−8.00 (0.15)	−6.97 (0.18)	−6.66
XIAP–AVPY	−7.16 (0.36)	−8.63 (0.35)	−7.20 (0.37)	−8.95
XIAP–AVPE	−7.23 (0.17)	−7.98 (0.17)	−7.24 (0.18)	−5.53
correlation coeff	0.10	0.58	0.23	

<sup>a</sup> All values are in kcal/mol units.

**Table 4.** Correlation Coefficients of Alternative Scores

	HPScore	HMScore	HSScore	XSCORE
maximum score	0.25	0.61	0.01	0.32
minimum score	0.13	0.60	0.30	0.18
minimized score	0.34	0.39	0.12	0.28

the most active peptides. However, if we do not take into account the XIAP–Smac/DIABLO(9) complex, HMScore suggests a value of  $\Delta G_{\text{HMScore}}$  greater than 8.00 kcal/mol to separate the most active from the least active peptides. The AVPY peptide is now predicted to have the highest affinity. This behavior of XSCORE can be attributed to the inherent flexibility of the lateral chains in the peptides that are not always present in organic molecules and the fact that XSCORE always gives close binding energies.

So far we have tested the average XSCORE data throughout the molecular dynamics, but we wanted to suggest other alternatives to this methodology. Table 4 shows the correlation coefficients taking into account the maximum and the minimum scores, both obtained along the molecular dynamic trajectory and the score obtained only from the minimization step, before the molecular dynamics simulation. Detailed values are not shown except for HMScores in Table 5, which is the best again. Here, using the maximum score, we have an improved correlation coefficient of 0.61 (Figure 4a shows a plot of the experimental binding free energy versus this alternative HMScore function). In this case, if we do not take into account the XIAP–Smac/DIABLO(9) complex, HMScore suggests a value of  $\Delta G_{\text{HMScore}}$  greater than 8.50 kcal/mol to separate most active peptides from least active ones. On the other hand, the minimized score, which is a cheap computational option, performs a third of all scores if we use the HM function. Moreover, the correlation coefficient decreases to 0.39, and it is not able to distinguish between the most and the least active peptides.

To achieve a much better XSCORE function it would be desirable to recalibrate some of the terms, particularly the rotor penalty, that is too large for the Smac/DIABLO(9 residues) peptide because the C-terminal part of this peptide is far from the binding pocket, and consistently some of the bonds are free rotors. In fact, the rotor for this peptide should be about 7 instead of 24 like the rotor in the AVPI peptide. If we change the rotor penalty in the Smac/DIABLO(9 residues) peptide to 7, it achieves the best score of all peptides, HPScore 5.65, HMScore 7.39, HSScore 5.85, and XSCORE of 6.30 (−8.64 kcal/mol). Now, this binding energy is close to the experimental one, but it is too high with respect to the other peptides so it does not improve the correlation.

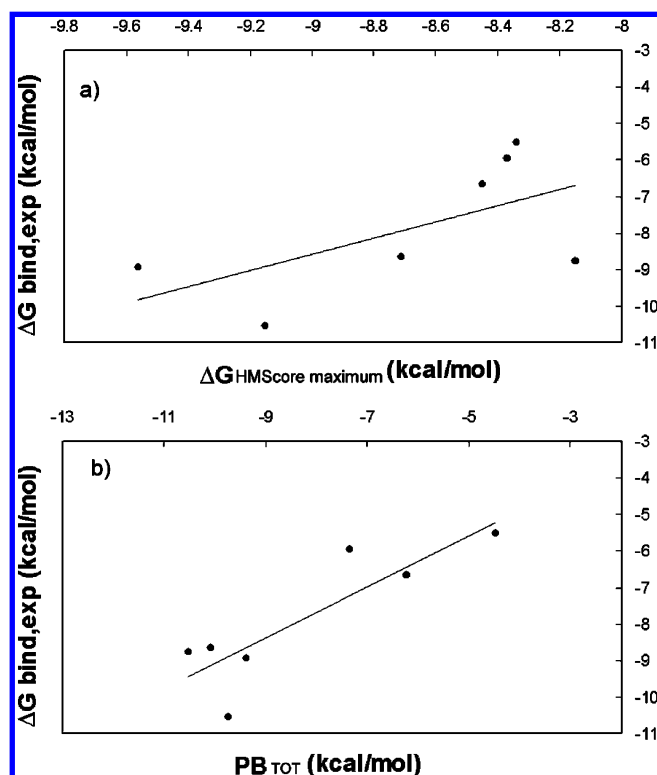
It is worth to note that, within the XSCORE framework, entropy variations are supposed to be included in both the rotor and the constant terms. However, in the MMPBSA context, if absolute binding free energies are required, the entropic contribution must be determined in order to obtain meaningful results. Unfortunately, this value is extremely difficult to calculate because of the computational cost of normal mode calculations. To get around this problem we should discuss relative binding free energies because in this case the entropic term is often assumed to cancel,<sup>5</sup> as it would have to be in our context, being that our peptides are similar molecules in the same binding pocket.

Having this fact in mind, we will discuss our results without the inclusion of the entropic contribution, and finally we will show how our results are affected by its inclusion.

Table 6 shows the average results (in kcal/mol) of the binding free energy calculations and the different energy contributions when applying the MMPBSA methodology, without the entropic contribution included. ELE accounts for the electrostatic interactions between the protein and the peptides that are responsible for large distance molecular recognition, VDW denotes van der Waals interactions between the fragments, that are related to complementary volume, and GAS accounts for the addition ELE+VDW+INT being the binding enthalpic contributions in vacuo. However, INT binding enthalpy, the balance of internal energy of the system, is always zero due to the one-trajectory protocol used in this work. PB<sub>SUR</sub> accounts for the nonpolar contribution to solvation related to SASA, being always binding favorable, PB<sub>CAL</sub> is the polar contribution of solvation, being in all cases unfavorable to binding, and PB<sub>SOL</sub> denotes the PB<sub>SUR</sub> + PB<sub>CAL</sub> addition related to the balance of solvation total contribution. PB<sub>ELE</sub> accounts for the PB<sub>CAL</sub> + ELE addition,

**Table 5.** Binding Free Energies of the Maximum, Minimum, and Minimized HMScores<sup>a</sup>

	$\Delta G_{\text{HMScore maximum}}$	$\Delta G_{\text{HMScore minimum}}$	$\Delta G_{\text{HMScore minimized}}$	$\Delta G_{\text{bind,exp}}$
XIAP–Smac/DIABLO(9res)	−8.15	−7.34	−7.61	−8.78
XIAP–AVPI	−8.71	−8.08	−9.08	−8.67
XIAP–ARPF	−9.15	−7.67	−8.81	−10.56
XIAP–AGPI	−8.37	−6.97	−8.24	−5.95
XIAP–AVPA	−8.45	−7.60	−8.50	−6.66
XIAP–AVPY	−9.56	−7.93	−9.56	−8.95
XIAP–AVPE	−8.34	−7.32	−8.23	−5.53

<sup>a</sup> All values are in kcal/mol units.**Figure 4.** Plots of experimental binding free energy versus the maximum HMScore of XSCORE methodology (a) and versus the  $PB_{\text{TOT}}$  of MMPBSA methodology (b).

that is, the balance of favorable electrostatic interactions between the fragments and unfavorable desolvation of them. It is always a negative binding factor showing how crucial van der Waals recognition is. Finally,  $PB_{\text{TOT}}$  accounts for the total binding free energy calculated by the MMPBSA method, and  $\Delta G_{\text{bind,exp}}$  is the experimental binding free energy at 300 K, for comparison.

MMPBSA shows a good performance, being the maximum error of 1.74 kcal/mol for the Smac/DIABLO(9 residues) ligand and the correlation coefficient of 0.86 (Figure 4b shows a plot of the experimental binding free energy versus the results obtained with the MMPBSA scoring function). Moreover, it is able to separate high affinity from bad affinity ligands (AGPI, AVPA, and AVPE). A  $PB_{\text{TOT}}$  around 7.5 kcal/mol can be selected as a limiting value. However, ARPF which is the ligand with the highest electrostatic interaction with the XIAP protein and the most active peptide does not appear as the first. This peptide is a charged ligand, and, as it has been noted previously, the use of a continuum electrostatic approach underestimates charged relative to zwitterionic ligands.<sup>36–39</sup> This fact is identifiable also in the AVPE peptide, with negative charge.

AVPA is the ligand with the lowest van der Waals interaction, and AVPE is the ligand with the lowest electrostatic interactions (followed by AGPI), these being two factors responsible for the poor affinity of both peptides.  $PB_{\text{SUR}}$  values are almost the same for each ligand, and  $PB_{\text{CAL}}$  is the bottleneck feature of binding affinity.

It is also interesting to study the influence of each mutation with respect to the original nine residues Smac/DIABLO sequence. By simply cutting the C-terminus, the AVPI peptide is obtained. This compound remains very active revealing the lack of interactions in this zone and confirming the point of view that AVPI is a conserved tetrapeptide motif and enough for binding. The mutation to glycine in the second position brings us the AGPI peptide. This peptide has few van der Waals and electrostatic interactions with the receptor. Thus, the valine in the second position gives hydrophobic contacts plus electrostatic ones, presumably placing correctly the hydrogen-bonding suggested experimentally.<sup>17</sup>

The AVPA peptide allows us to notice the influence of mutations at the fourth position. Mutation to alanine implies that the van der Waals interactions will decrease around 5 kcal/mol. In fact this is the most pronounced change, being that this position is extremely important to hydrophobic recognition of both fragments.

In the same way, the glutamic acid in the AVPE peptide decreases the electrostatic interaction with the receptor being the peptide with the lowest affinity.

The AVPY peptide allows us to notice the influence of a large residue in the fourth position. Binding affinity does not change substantially with respect to the AVPI sequence, so we can see that the fourth position can allocate large and not flexible fragments like the tyrosine side chain.

Finally ARPF has two point mutations, clearly the charged arginine at the second position increases the electrostatic contacts to −302.32 kcal/mol revealing the negative charge of the BIR3 domain of XIAP, but then the desolvation contribution is also more unfavorable, and maybe the MMPBSA notes this in extreme when using parse radii.<sup>40</sup> Phenylalanine at the fourth position increases the van der Waals contribution to binding more than tyrosine so the affinity increases with a large, completely apolar and not flexible residue like phenylalanine. Recognition of ARPF involves the higher electrostatic interaction of all peptides and the higher van der Waals interaction of all tetrapeptides.

$\Delta G_{\text{bind}}$  values, accounting for entropic contributions, are shown in Table 7, in kcal/mol units. As we stated before, introduction of entropic contributions is one of the more difficult aspects of the MMPBSA approximation. For this reason, we have analyzed the influence of usual approximations introduced in its calculation in order to reduce the



**Table 6.** Average Data of MMPBSA Methodology<sup>a</sup>

	ELE	VDW	GAS	PB <sub>SUR</sub>	PB <sub>CAL</sub>	PB <sub>SOL</sub>	PB <sub>ELE</sub>	PB <sub>TOT</sub>	$\Delta G_{\text{bind,exp}}$
XIAP–Smac/DIABLO(9res)	−179.57	−36.29	−215.86	−4.48	209.81	205.34	30.24	−10.52 (1.32)	−8.78
XIAP–AVPI	−154.41	−31.58	−185.99	−3.94	179.86	175.92	25.45	−10.07 (0.88)	−8.67
XIAP–ARPF	−302.32	−33.45	−335.76	−4.34	330.37	326.02	28.05	−9.74 (0.95)	−10.56
XIAP–AGPI	−139.27	−30.69	−169.96	−4.21	166.82	162.61	27.55	−7.35 (1.13)	−5.95
XIAP–AVPA	−146.17	−25.15	−171.31	−3.58	168.66	165.08	22.49	−6.23 (1.36)	−6.66
XIAP–AVPY	−174.42	−28.38	−202.80	−3.80	197.21	193.41	22.80	−9.39 (0.89)	−8.95
XIAP–AVPE	−124.74	−30.76	−155.50	−4.42	155.44	151.02	30.70	−4.48 (1.00)	−5.53

<sup>a</sup> ELE accounts for the electrostatic interactions, VDW denotes the van der Waals interactions between the fragments, GAS accounts for the addition ELE+VDW+INT being the binding enthalpic contributions in vacuo, PB<sub>SUR</sub> accounts for the nonpolar contribution to solvation, PB<sub>CAL</sub> is the polar contribution of solvation, PB<sub>SOL</sub> denotes the PB<sub>SUR</sub> + PB<sub>CAL</sub>, PB<sub>ELE</sub> accounts for the PB<sub>CAL</sub> + ELE addition, PB<sub>TOT</sub> accounts for the total binding free energy calculated by the MMPBSA method with its standard error in brackets, and  $\Delta G_{\text{bind,exp}}$  is the experimental binding free energy. All values are in kcal/mol units.

**Table 7.** Inclusion of Entropy in MMPBSA Methodology<sup>a</sup>

	$T\Delta S_{\text{TRAS}}$	$T\Delta S_{\text{ROT}}$	$T\Delta S_{\text{VIB}}$	$T\Delta S_{\text{TOT}}$	$\text{PB}_{\text{TOT}} - T\Delta S_{\text{TOT}}$	$\Delta G_{\text{bind,exp}}$
XIAP–Smac/DIABLO(9res)	−13.85	−12.38	−6.65 (2.11)	−32.79 (2.11)	22.27	−8.78
XIAP–AVPI	−13.12	−10.91	7.80 (3.75)	−16.23 (3.77)	6.16	−8.67
XIAP–ARPF	−13.30	−11.27	−2.18 (2.36)	−26.75 (2.37)	17.01	−10.56
XIAP–AGPI	−13.02	−10.81	3.35 (1.03)	−20.48 (1.04)	13.13	−5.95
XIAP–AVPA	−13.02	−10.69	1.49 (5.31)	−22.22 (5.32)	15.99	−6.66
XIAP–AVPY	−13.22	−11.17	2.50 (4.41)	−21.89 (2.19)	12.50	−8.95
XIAP–AVPE	−13.15	−10.99	7.24 (4.55)	−16.90 (4.54)	12.42	−5.53

<sup>a</sup> Eight snapshots were used for the first complex and five for the other ones,  $T\Delta S_{\text{TRAS}}$  is the translation entropy,  $T\Delta S_{\text{ROT}}$  accounts for the rotational entropy,  $T\Delta S_{\text{VIB}}$  denotes the vibrational entropy with its standard error in brackets,  $T\Delta S_{\text{TOT}}$  accounts for the addition  $T\Delta S_{\text{TRAS}} + T\Delta S_{\text{ROT}} + T\Delta S_{\text{VIB}}$ ,  $\text{PB}_{\text{TOT}} - T\Delta S_{\text{TOT}}$  is the final free energy of binding, and  $\Delta G_{\text{bind,exp}}$  is the experimental binding free energy. All values are in kcal/mol units.

computational complexity. The first factor considered was the size of the subsystem used to simulate the whole system. The results in Table 7 have been obtained using the complete system because in our case this is computationally feasible. This is however an important factor, as can be seen from the results of the XIAP–Smac/DIABLO complex taken as a representative example. In this case, using a 12 Å cutoff value that includes 33 neighboring residues of the smac peptide, the calculated  $T\Delta S$  value is −26.26 kcal/mol. Comparing with the full system result (Table 7), we obtain a difference of 6.53 kcal/mol arising basically from the vibrational entropy contribution, being  $T\Delta S_{\text{vib}}$  −6.56 kcal/mol for the full system and −0.41 kcal/mol for the truncated one. Thus, selection of the appropriate cutoff is of great importance. The fact that vibrational entropy is the determinant part of the computed total entropy can be deduced easily from results reported in Table 7, where contributions coming from translational and rotational entropy are mainly constant among all the complexes. Another computational input in MMPBSA calculations is the value of the gradient root-mean-square deviation (rmsd) considered in the minimization procedure. Its value was set to  $10^{-4}$  kcal/mol Å for all calculations in this work. However, its change to  $10^{-5}$  kcal/mol Å did not produce any appreciable modification of the calculated entropic contribution. The last aspect studied here related to the entropy calculation is the number of snapshots used for its statistical treatment. To see how important is this number in the final entropic values, we performed three different calculations using 5, 10, and 20 snapshots extracted equally spaced from the production time for the XIAP–AVPA complex, which was selected as an example because of its high deviation of  $T\Delta S_{\text{vib}}$ . The obtained values for the vibrational contribution were 1.49, 3.02, and 1.27 kcal/mol with standard errors of 5.31, 2.77, and 1.67,

respectively. As can be seen, convergence is similar to that usually observed for  $\Delta G$  values, having a stable value for a reduced number of snapshots. The other two entropic contributions are approximately constant, and the same general behavior was observed for all the other systems.

## CONCLUSIONS

In the present work, molecular dynamics simulations and binding free energies estimations of seven XIAP–peptide complexes with biological relevance in cancer disease have been performed. In order to determine their binding free energies, 100 snapshots from each 1 ns molecular dynamics simulation were extracted and analyzed by XSCORE<sup>8</sup> and MMPBSA<sup>5</sup> methodologies.

XSCORE was originally developed to treat large ligand databases with rigid receptors structures without the need for a previous molecular dynamics run and without the need for addition of hydrogen atoms which are not present in crystal structures. However, we wanted to test this methodology in the same conditions as MMPBSA performs, that is, with a set of representative structures of each system, and using the same target with seven similar peptidic ligands.

Regarding the results, XSCORE was able to predict the binding free energy with a maximum error of 3 kcal/mol although with a very small correlation coefficient of 0.02. This value was substantially improved to 0.61 when using the HMScore function and maximum scores.

Although more work should need to be done in different systems to corroborate our results, the worst aspect of XSCORE was the ineffectiveness of identifying good and bad peptide inhibitors of XIAP in a large range of activity. This fact can be attributed to the mobility of peptide lateral chains during the molecular dynamics that is not reflected

in the XSCORE values, putting all the conformations in a close binding energy range. One can overcome this fact, at least in part, by using our suggested maximum score together with the HMScore function. Nevertheless, taking into account these guidelines and the fact that this method is computationally very cheap, it can be a good choice to evaluate binding free energies as a first step in drug design. However, as indicated by the XIAP–Smac/DIABLO(9) complex results, it seems necessary to recalibrate some terms of the score function to take into account the existence of peptide residues that do not interact directly with the receptor.

MMPBSA is clearly a more robust method, and, in the particular case of these XIAP–peptide complexes, it predicted binding free energies in an accurate manner when no entropic contribution is added, being able to identify slight binding differences with a maximum error of 1.7 kcal/mol and a good correlation coefficient of 0.86. In this sense, MMPBSA can be used as a good scoring function, when only relative binding is important.

Unfortunately, in our case, the addition of entropic contributions moves the absolute binding free energies to positive values decreasing dramatically the correlation coefficient. As the total free energy is obtained with the addition of  $PB_{TOT}$  to the entropy, we could obtain negative bindings modifying the former contribution. For some authors the positive values of the total free energy of binding were mainly attributed to the use of parse radii instead of bondi radii<sup>40</sup> for the resolution of the Poisson–Boltzmann equation. Parse radii are smaller than bondi radii, which is translated into a higher desolvation penalty and smaller  $PB_{TOT}$  results. For other authors it was a consequence of the standard and different protocols used for MMPBSA calculations.<sup>41</sup>

However, none of the methods is capable of answering why the ARPF ligand is so active, even more active than the original nine-residue sequence of Smac/DIABLO. It is difficult to understand this activity, and a crystal structure of ARPF in complex with XIAP would be of great help.

On the other hand, it is worth noting that we used experimental initial coordinates only for the first system, and the MMPBSA results for this one and for the other systems, modeled by homology, were correctly correlated to experimental data, indicating that active biological conformations have been located.

Finally we should point out that absolute correlation coefficients should be taken with caution given that there are only seven points in the regression.

Regarding the cationic dummy approach<sup>18</sup> for the treatment of the metal atom in XIAP, it was a proper choice because the four coordination of the zinc was maintained over the whole simulation with correct distances from the protein atoms. We think that the same methodology used to develop force field parameters for the zinc can be extrapolated, with necessary changes, to other metalloproteins.

#### ACKNOWLEDGMENT

We are grateful to the CEPBA-IBM Research Institute for a generous allocation of computer time, granted to the project *Design of new antitumoral drugs by means of molecular modeling tools*. The Spanish Ministry of Science and Technology supported this work through grant number CTQ2006-06588/BQU. We want to thank Dr. Jose Manuel

Granadino for his careful reading of the manuscript. We also are thankful for the support of the Departament d'Universitats, Recerca i Societat de la informació de la Generalitat de Catalunya i del Fons Social Europeu.

#### REFERENCES AND NOTES

- (1) Stites, W. E. Protein-protein interactions: Interface structure, binding thermodynamics, and mutational analysis. *Chem. Rev.* **1997**, *97*, 1233–1250.
- (2) Jain, R.; Ernst, J.; Kutzki, O.; Park, H. S.; Hamilton, A. D. Protein recognition using synthetic surface-targeted agents. *Mol. Divers.* **2004**, *8*, 89–100.
- (3) Kollman, P. A. Free energy calculations: applications to chemical and biochemical phenomena. *Chem. Rev.* **1993**, *93*, 2395–2417.
- (4) Carlson, H. A.; Jorgensen, W. L. An extended linear response method for determining free energies of hydration. *J. Phys. Chem.* **1995**, *99*, 10667–10673.
- (5) Kollman, P. A.; Massova, I.; Reyes, C.; Kuhn, B.; Huo, S.; Chong, L.; Lee, M.; Lee, T.; Duan, Y.; Wang, W.; Donini, O.; Srivasan, J.; Case, D. A.; Cheatham, T. E., III. Calculating structures and free energies of complex molecules: Combining molecular mechanics and continuum models. *Acc. Chem. Res.* **2000**, *33*, 889–897.
- (6) Gohlke, H.; Kiel, C.; Case, D. A. Insights into protein-protein binding by binding free energy calculation and free energy decomposition for the Ras-Raf and Ras-RalGDS complexes. *J. Mol. Biol.* **2003**, *330*, 891–913.
- (7) Gouda, H.; Kuntz, I. D.; Case, D. A.; Kollman, P. A. Free energy calculations for theophylline binding to an RNA aptamer: Comparison of MM-PBSA and thermodynamic integration methods. *Biopolymers* **2003**, *68*, 16–34.
- (8) Wang, R.; Lai, L.; Wang, S. Further development and validation of empirical scoring functions for structure-based binding affinity prediction. *J. Comput.-Aided Mol. Des.* **2002**, *16*, 11–26.
- (9) Wang, R.; Lu, Y.; Wang, S. Comparative evaluation of 11 scoring functions for molecular docking. *J. Med. Chem.* **2003**, *46*, 2287–2303.
- (10) Shiraki, K.; Sugimoto, K.; Yamanaka, Y.; Yamaguchi, Y.; Saitou, Y.; Ito, K.; Yamamoto, N.; Yamanaka, T.; Fujikawa, K.; Murata, K.; Kano, T. Overexpression of x linked inhibitor of apoptosis protein in human hepatocellular carcinoma. *Int. J. Mol. Med.* **2003**, *12*, 705–708.
- (11) Tamm, I.; Kornblau, S. M.; Segall, H.; Krajewski, S.; Welsh, K.; Kitada, S.; Scudiero, D. A.; Tudor, G.; Qui, Y. H.; Monks, A.; Andreeff, M.; Reed, J. C. Expression and Prognostic Significance of IAP-Family Genes in Human Cancers and Myeloid Leukemias. *Clin. Cancer Res.* **2000**, *6*, 1796–1803.
- (12) Yang, X.; Xing, H.; Gao, Q.; Chen, G.; Lu, Y.; Wang, Y.; Ma, D. Regulation of HtrA2/Omi by X-linked inhibitor of apoptosis protein in chemoresistance in human ovarian cancer cells. *Gynecol. Oncol.* **2005**, *97*, 413–421.
- (13) Kipp, R. A.; Case, M. A.; Wist, A. D.; Cresson, C. M.; Carrell, M.; Griner, E.; Wiita, A.; Albinia, P. A.; Chai, J.; Shi, Y.; Semmelhack, F.; McLendon, G. L. Molecular targeting of inhibitor of apoptosis proteins based on small molecule mimics of natural binding partners. *Biochemistry* **2002**, *41*, 7344–7349.
- (14) Glover, C. J.; Hite, K.; DeLosh, R.; Scudiero, D. A.; Fivash, M. J.; Smith, L. R.; Fisher, R. J.; Wu, J.; Shi, Y.; Kipp, R. A.; McLendon, G. L.; Sausville, E. A.; Shoemaker, R. H. A high-throughput screen for identification of molecular mimics of Smac/DIABLO utilizing a fluorescence polarization assay. *Anal. Biochem.* **2003**, *320*, 157–169.
- (15) Schimmer, A. D.; Welsh, K.; Pinilla, C.; Wang, Z.; Krajewska, M.; Bonneau, M.; Pedersen, I. M.; Kitada, S.; Scott, F. L.; Bailly-Maitre, B.; Glinsky, G.; Scudiero, D.; Sausville, E.; Salvesen, G.; Nefzi, A.; Ostresh, J. M.; Houghten, R. A.; Reed, J. C. Small-molecule antagonists of apoptosis suppressor XIAP exhibit broad antitumor activity. *Cancer Cell* **2004**, *5*, 25–35.
- (16) Oost, T. K.; Sun, C.; Armstrong, R. C.; Al-Assaad, A.; Betz, S. F.; Deckwerth, T. L.; Ding, H.; Elmore, S. W.; Meadows, R. P.; Olejniczak, E. T.; Oleksijew, A.; Oltersdorf, T.; Rosenberg, S. H.; Shoemaker, A. R.; Tomaselli, K. J.; Zou, H.; Fesik, S. W. Discovery of potent antagonists of the antiapoptotic protein XIAP for the treatment of cancer. *J. Med. Chem.* **2004**, *47*, 4417–4426.
- (17) Liu, Z.; Sun, C.; Olejniczak, E.; Meadows, R.; Betz, S.; Oost, T.; Herrmann, J.; Wu, J.; Fesik, S. Structural basis for binding of Smac/DIABLO to the XIAP BIR3 domain. *Nature* **2000**, *408*, 1004–1008.
- (18) Pang, Y. P.; Xu, K.; El Yazla, J.; Prendergast, F. Successful molecular dynamics simulation of the zinc-bound farnesyltransferase using the cationic dummy atom approach. *Protein Sci.* **2000**, *9*, 1857–1865.



- (19) Pang, Y. P. Novel zinc protein molecular dynamics simulations: steps towards antiangiogenesis for cancer treatment. *J. Mol. Model.* **1999**, 5, 196–202.
- (20) Pang, Y. P. Successful molecular dynamics simulation of two zinc complexes bridged by a hydroxide in phosphotriesterase using the cationic dummy atom method. *Proteins* **2001**, 45, 183–189.
- (21) Oelschlaeyer, P.; Schmid, D. R.; Pleiss, J. Insight into the mechanism of the IMP-1 metallo- $\beta$ -lactamase by molecular dynamics simulations. *Protein Eng.* **2003**, 16, 341–350.
- (22) Jorgensen, W. L.; Chandrosskhar, J.; Madura, J.; Impey, R.; Klein, M. Comparison of simple potential functions for simulating liquid water. *J. Chem. Phys.* **1983**, 79, 926–935.
- (23) Cornell, W. D.; Cieplak, P.; Bayly, C. I.; Goud, I. R.; Mertz, K. M., Jr.; Ferguson, D. M.; Spellmeyer, D. C.; Fox, T.; Caldwell, J. W.; Kollman, P. A. A second generation of force fields for the simulation of proteins, nucleic acids and organic molecules. *J. Am. Chem. Soc.* **1995**, 117, 5179–5197.
- (24) Case, D. A.; Pearlman, D. A.; Caldwell, J. W.; Cheatham, T. E., III; Wang, J.; Ross, W. S.; Simmerling, C. L.; Darden, T. D.; Merz, K. M.; Stanton, R. V.; Cheng, A. L.; Vincent, J. J.; Crowley, M.; Tsui, V.; Gohlke, H.; Radmer, R. J.; Duan, Y.; Pitera, J.; Massova, I.; Seibel, G. L.; Sligh, U. C.; Weiner, P. K.; Kollman, P. A. AMBER 7; University of California: San Francisco, CA, 2002.
- (25) Darden, T.; York, D.; Pedersen, L. Particle mesh Ewald: an  $N \log(N)$  method for Ewald sums in large systems. *J. Chem. Phys.* **1993**, 98, 10089–10092.
- (26) Berendsen, H. J. C.; Postman, J. P. M.; Van Gunsteren, W. F.; DiNola, A.; Haak, J. A. Molecular dynamics with coupling to an external bath. *J. Chem. Phys.* **1984**, 81, 3684–3690.
- (27) Ryckaert, J. P.; Ciccotti, G.; Berendsen, H. J. Numerical integration of the cartesian equations of motion of a system with constraints: molecular dynamics of n-alkanes. *J. Comput. Chem.* **1977**, 23, 327–341.
- (28) Srinivasan, J.; Cheatham, T. E.; Cieplak, P.; Kollman, P. A.; Case, D. A. Continuum solvent studies of the stability of DNA, RNA and phosphoramidate-DNA helices. *J. Am. Chem. Soc.* **1998**, 120, 9401–9409.
- (29) Bashford, D.; Gerwent, K. Electrostatic calculations of the pKa values of ionizable groups in bacteriorhodopsin. *J. Mol. Biol.* **1992**, 224, 473–486.
- (30) Nicholls, A.; Honing, B. A rapid finite difference algorithm, utilizing successive overrelaxation to solve the Poisson-Boltzmann equation. *J. Comput. Chem.* **1991**, 12, 435–445.
- (31) Sitkoff, D.; Sharp, K.; Honing, B. Accurate calculations of hydration free energies using macroscopic solvents. *J. Phys. Chem.* **1994**, 98, 1978–1988.
- (32) Weiser, J.; Shemkin, P. S.; Still, W. C. Approximate atomic surfaces from linear combinations of pairwise overlaps (LCPO). *J. Comput. Chem.* **1999**, 20, 217–230.
- (33) Sigfridsson, E.; Ryde, U. Comparison of methods for deriving atomic charges from the electrostatic potential and moments. *J. Comput. Chem.* **1997**, 19, 377–395.
- (34) Hoops, S. C.; Anderson, K. W.; Merz, K. M. Force field design for metalloproteins. *J. Am. Chem. Soc.* **1991**, 113, 8262–8270.
- (35) Wang, R.; Lu, Y.; Fang, X.; Wang, S. An extensive test of 14 scoring functions using the PDBbind refined set of 800 protein-ligand complexes. *J. Chem. Inf. Comput. Sci.* **2004**, 44, 2114–2125.
- (36) Bonnet, P.; Bryce, R. A. Scoring binding affinity of multiple ligands using implicit solvent and a single molecular dynamics trajectory: application to influenza neuraminidase. *J. Mol. Graphics Modell.* **2005**, 24, 147–156.
- (37) Bonnet, P.; Bryce, R. A. Molecular dynamics and free energy analysis of neuraminidase–ligand interactions. *Protein Sci.* **2004**, 13, 946–957.
- (38) Smith, B. J.; Colman, P. M.; von Itzstein, M.; Daylec, B.; Varghese, J. N. Analysis of inhibitor binding in influenza virus neuraminidase. *Protein Sci.* **2001**, 10, 689–696.
- (39) Taylor, N. R.; von Itzstein, M. A structural and energetics analysis of the binding of a series of N-acetylneuraminic-acid-based inhibitors to influenza virus sialidase. *J. Comput.-Aided Mol. Des.* **1996**, 10, 233–246.
- (40) Gohlke, H.; Case, D. A. Converging free energy estimates: MM-PB-(GB)SA studies on the protein-protein complex Ras-Raf. *J. Comput. Chem.* **2004**, 25, 238–250.
- (41) Pearlman, D. A. Evaluating the molecular mechanics Poisson-Boltzmann surface area free energy method using a cogenetic series of ligands to p38 MAP kinase. *J. Med. Chem.* **2005**, 48, 7796–7806.

CI600412Z